Research Article Vol. 2, No. 6 / 15 June 2019 / OSA Continuum 1917

OSA CONTINUUM

Electronic holographic three-dimensional display with enlarged viewing angle using non-mechanical scanning technology

GUANGLIN YANG,[1,*] WEIHAO HAN,[1] TAOMIN XIE,[1] AND HAIYAN XIE[2]

[1] Laboratory of Signal and Information Processing, Department of Electronics, School of Electronic Engineering and Computer Science, Peking University, Beijing 100871, China
[2] China Science Patent and Trademark Agent, Beijing 100083, China
[*] ygl@pku.edu.cn

Abstract: A non-mechanical scanning method based on a liquid-crystal spatial light modulator (LC-SLM) is proposed to increase the viewing angle of electronic holographic three-dimensional (3D) displays. A scanning off-axis Fresnel lens is simulated by the LC-SLM to deflect the reconstructed light beam. Using the time-division multiplexing method, the viewing zones are sequentially projected to different positions. When the eyes of the observer are located at the viewing zones, the reconstructed 3D images can be observed. The experimental results and analyses show the feasibility and advantages of the proposed method.

1. Introduction

Electronic holography is of importance in three-dimensional (3D) displays [1]. As the electronic holography can record the amplitude and phase information of an object, it can display real 3D information of objects, as a naked-eye 3D display technology. However, the electronic holography is limited by materials and technology, the narrow viewing angle being one of the major challenges. Several methods have been proposed, in order to increase the viewing angle of the electronic holographic 3D displays, which can be divided into two categories.

The first category of methods is based on space-division multiplexing with multiple spatial light modulators (SLMs). The multiple SLMs are arranged linearly, and the reconstructed images are spliced. An electronic holographic 3D display system with broad viewing angles can be obtained. Finke employed multiple charge-coupled device (CCD) cameras on a curved surface to record the multiple digital holograms, and used multiple liquid-crystal (LC) SLMs to splice the viewing zones [2]. Hahn arranged 12 SLMs into a curved array, to extend the viewing angles to 22.8° [3]. This method can efficiently increase the viewing angle of the electronic holographic 3D display. However, it is very expensive.

The second category of methods is based on time division multiplexing (TDM) with a single SLM. Chen used three mirrors to splice the sub-holograms in different viewing zones in order to expand the viewing angles [4]. Liu employed linear phase superposition to construct an equivalent SLM array, which can increase the viewing angles of the electronic holographic 3D display by 3.6 times [5]. However, the optical path of splicing the sub-holograms at different moments is complex and flicker is easy to occur. Mechanical scanning technology has been also employed to increase the viewing angles. Teng combined a Fourier-transform holographic display system and rotating tilt mirror to achieve a 360° electronic holographic 3D display [6]. Kim used Fresnel holography with a rotating ellipsoidal mirror to expand the viewing angle [7]. Takaki used a digital micromirror device (DMD) to load the point-source-based holograms and rotating off-axis Fresnel reflector as a display desktop, to develop a naked-eye 360° holographic 3D display [8]; the viewing zones were located in a fixed circle that limits the viewing effect. This method has high requirements for the mechanical control of the scanning system. The

#363401 https://doi.org/10.1364/OSAC.2.001917
Journal © 2019 Received 26 Mar 2019; revised 15 May 2019; accepted 16 May 2019; published 3 Jun 2019

OSA CONTINUUM

mechanical rotation speed of the mirror needs to be consistent with the refresh frequency of the spatial light modulator, otherwise it is prone to image crosstalk.

In this study, we propose a non-mechanical scanning method based on an LC-SLM to increase the viewing angle of the electronic holographic 3D display. A scanning off-axis Fresnel lens is simulated by the LC-SLM to deflect the reconstructed light beam. Using the TDM method, the viewing zones are sequentially projected to different positions. People can see the reconstructed 3D images at an increased viewing angle.

2. Non-mechanical scanning technology based on LC-SLM

In this study, a non-mechanical scanning method based on an LC-SLM is proposed in order to increase the viewing angle of the electronic holographic 3D display system [12]. Each pixel of LC-SLM is composed of liquid crystal molecule and electronic control device. According to the characteristic curve of deflection angle of liquid crystal molecule changing with external electric field voltage, the liquid crystal molecule of LC-SLM is loaded with external electric field voltage, so that each pixel unit modulates the incident light phase [13,14].

Two experimental methods have been employed to achieve beam deflection based on an LC-SLM, blazed grating [15] and off-axis Fresnel lens [16] methods. The off-axis Fresnel lens method produces an off-axis lens wavefront by diffraction, which controls the angle of beam deflection by the position of the lens axis. In this study, the off-axis Fresnel lens method is used to simulate an off-axis Fresnel lenses illustrated in Fig. 1.

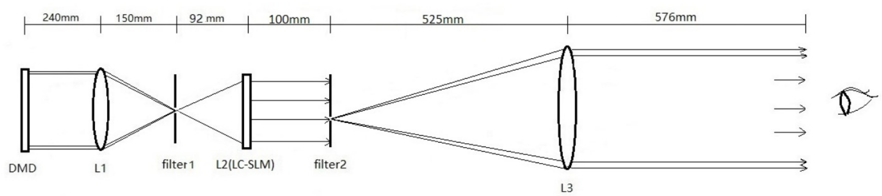

Fig. 1. Three-lens optical system for an electronic holographic 3D display.

In Fig. 1, L1 is a projection lens. The spatial filters are placed on the back focal plane of L1 and L2 to filter out the zero-order and high-order diffractions waves. An LC-SLM simulates an L2 lens. By loading the corresponding phase diagram to change the position of the lens axis simultaneously, we can control the angle of beam deflection. L3 is an imaging lens that magnifies images. Without L3, the size of the reconstructed images would be limited.

Fig. 2 shows beam deflection with all-positive decentered macroscopic lenses. A simple beam steering system consists of the first lens and the third lens. The second lens is the field lens, which reduces the light loss of the system due to vignetting when the beam of light is steered off-axis [19].

The decentered lens group shows the working principle of the off-axis Fresnel lens methods of LC-SLM. The algorithm of beam deflection can be understood by moving first single positive lens [18], as shown in Fig. 2. The scanning range of the beam depends on the lens displacement Δ, which will lead to a deflection angle θ.

According to the principle of phase modulation of LC-SLM, the transmittance function of a thin lens at the near-axis condition can be expressed as:

$$t(x,y) = P(x,y)\exp\left[-j\frac{k}{2f}(x^2+y^2)\right] \tag{1}$$

where k is $2\pi/\lambda$, P(x, y) is the pupil function. If the light is within the aperture of the lens P(x, y) = 1, otherwise P(x, y) = 0. This function limits the size of the lens. In Eq. (1), the phase

OSA CONTINUUM

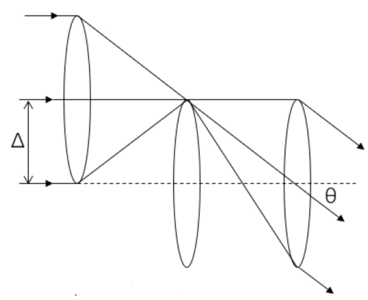

Fig. 2. Beam deflection with all-positive decentered macroscopic lenses.

factor which represents the modulation of the phase is:

$$\exp\left[-j\frac{k}{2f}(x^2+y^2)\right] \tag{2}$$

At the off-axis condition, the transmittance function can be rewritten as:

$$t(x,y) = P(x,y)\exp\left[-j\frac{k}{2f}((x-x_0)^2+(y-y_0)^2)\right] \tag{3}$$

Therefore, the phase function can be expressed as:

$$\varphi(x,y) = mod_{2\pi}\left(-\frac{\pi}{\lambda f_{slm}}((x-x_0)^2+(y-y_0)^2)\right) \tag{4}$$

where f_{slm} is the focal length of the equivalent lens, (x_0, y_0) is the position of the equivalent lens axis, λ is the wavelength of the incident light, and *mod* denotes the modulo function.

Using Eq. (4), the local spatial frequencies along the x- and y-axes can be expressed as:

$$\begin{cases} f_x = \frac{1}{2\pi}\frac{\partial\varphi}{\partial x} = \frac{1}{\lambda f_{slm}}|x-x_0| \\ f_y = \frac{1}{2\pi}\frac{\partial\varphi}{\partial y} = \frac{1}{\lambda f_{slm}}|y-y_0| \end{cases} \tag{5}$$

Limited by the pupil function, $(x-x_0)_{max} = \frac{N_x d}{2}$, $(y-y_0)_{max} = \frac{N_y d}{2}$. The maximum spatial frequency can be expressed as:

$$\begin{cases} f_{xmax} = \frac{1}{2\lambda f_{slm}}(N_x d) \\ f_{ymax} = \frac{1}{2\lambda f_{slm}}(N_y d) \end{cases} \tag{6}$$

where N_x and N_y denote the numbers of pixels of the LC-SLM in the x- and y-directions, respectively, λ is the wavelength of the incident light, and d is the size of the pixels. And f_{slm} is the focal length of the equivalent lens. According to the sampling theorem, maximum local spatial frequency of the Fresnel lens loaded by the phase-only LC-SLM should not be higher than the half of the reciprocal of the pixel interval of the LC-SLM; i.e.:

$$f_{slm} \geq \max\left(\frac{N_x d^2}{2\lambda}, \frac{N_y d^2}{2\lambda}\right) \tag{7}$$

The basic principle of the non-mechanical scanning technology based on LC-SLM by blazed grating method and off-axis Fresnel lens methods is to achieve mod 2π phase delay, which can

OSA CONTINUUM

vary the inclination of the incident light. As the minimum period of the LC discrete structure is 2 pixels, according to the grating equation [13], the maximum deflection angle obtainable with a spatial light modulator [20] can be expressed as:

$$\theta = \arcsin\frac{\lambda}{2d} \tag{8}$$

Equation (8) shows that when the pixel size of phase-only SLM is smaller, the deflection angle can be larger [12].

The gap between the sub-images based on the blazed grating method is conspicuous, and the jump interval is large. As the deflection angle increases, the diffraction efficiency of the reproduced light decreases. Therefore, we use the off-axis Fresnel lens methods to maximize the actual viewing angle and make the imaging clearer.

3. Beam deflection optical system with multiple views

The proposed method is aimed to increase the viewing angle of the electronic holographic 3D display. It consists of two parts; in the first part, holograms are generated using the point-source method at different viewing positions [9,10,11]; in the second part, an optical system (Fig. 1) is employed to increase the viewing angles of the electronic holographic 3D display.

In the first part, sub-holograms of multiple views of the object are generated. The point-source coordinate model of the object is produced in the 3D Cartesian coordinate system, and according to the point-source method, the holograms are calculated using a computer. In experiments, a novel look-up table method is employed to improve the efficiency of computer-generated hologram (CGH) computations. Its detail is described in References [10,11,17]. A series of sub-holograms with parallax is generated by translating the holographic recording plane, as illustrated in Fig. 3.

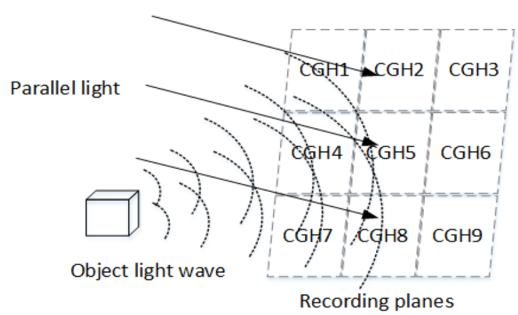

Fig. 3. Sub-holograms generated with multiple views.

In Fig. 3, the holograms are recorded at different viewing positions of the object. The reconstructed images are projected to the corresponding viewing areas using the beam-deflection optical system.

In the second part, an optical system (Fig. 1) is used to expand the viewing angle of the electronic holographic 3D display, as illustrated in Fig. 4.

In Fig. 4, the nine holograms are loaded by the DMD, and the sub-reconstructed images are sequentially generated. The corresponding phase diagrams of off-axis Fresnel lens are loaded by LC-SLM in sequence. The sub-reconstructed images are scanned by LC-SLM to project them to different viewing zones.

According to Eq. (4), the phase diagrams of off-axis Fresnel lenses with different axis positions are generated, the focal length of which is f_{slm}, and the axis position is (y_0, x_0). Different phase

OSA CONTINUUM

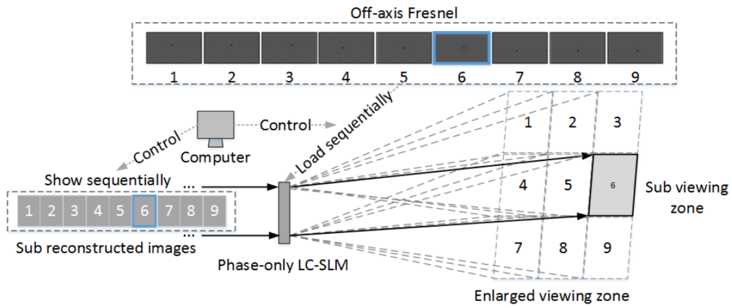

Fig. 4. Non-mechanical scanning employed to enlarge the viewing zone.

factors are added to the phase-only SLM to separate the diffraction in space. The corresponding images loaded by DMD and the phase diagrams loaded by LC-SLM are matched at any time.

In order to provide flicker-free image, the refresh rates of both DMD and LC-SLM in each viewing zone should be at least 50 Hz. Therefore, the display of both DMD and LC-SLM should be larger than 50×9 Hz to achieve nine viewing zones.

4. Experimental results and analysis

In the experiments, the 3D object is a cube box; each edge of the cube consists of 21 point light sources. On the top, left, and front faces of the cube, three letters ("PKU") are shown, composed of point light sources, as shown in Fig. 5(a).

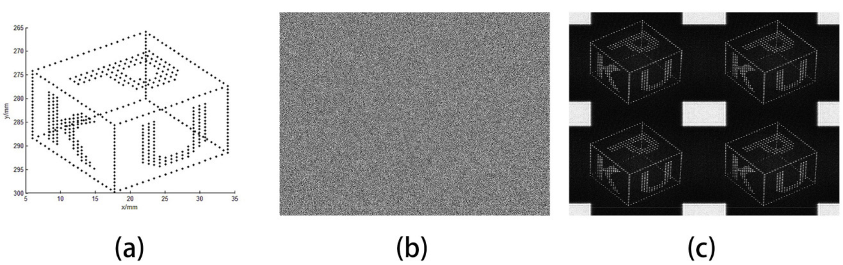

Fig. 5. "PKU" hologram generated and reconstructed using a computer. (a) 3D object consisting of point light sources, (b) computer generated holograms, and (c) simulation of reconstructed image.

The size of the object is $2\,cm \times 2\,cm \times 2\,cm$. The sampling interval between points is $1\,mm \times 1\,mm \times 1\,mm$. The number of pixels in the hologram is 1024×768; the sampling interval of the hologram is $13.7\ \mu\,m \times 13.7\ \ \mu\,m$. The wavelength of the incident light is 650 nm. The hologram is generated using the point-source method, as shown in Fig. 5(b). Computer simulation of the reconstructed image before filtering is shown in Fig. 5(c). There are higher-order diffractions, and the central white rectangle is the zero-order diffraction.

In the experiments, a phase-only LC-SLM provided by Holoeye is used to deflect the beam. The working area of the SLM is $15.36\,mm \times 8.64\,mm$, and the resolution is 1920×1080 pixels. The pixel size is 8 μ m, while the range of phase modulation is 2π. The frequency of the SLM is 60 Hz. We can only generate three viewing zones in the experiments; the refresh rate of each viewing zone is 20 Hz, which may cause some flicker. According to Eq. (7), the minimum focal length is 94.5 mm; it is set to 100 mm in the experiment. Light is reflected from DMD to SLM for imaging. The real image was displayed at the position of the LC-SLM by DMD. The distance between L1 and the DMD is 240 mm. The spatial filter is placed on the back focal plane of L1.

OSA CONTINUUM

The focal length of L1 and L3 are 150 mm and 300 mm, respectively. And in order to filter the zero-order spot and high-order diffraction generated by the Fresnel lens simulated by LC-LSM, another spatial filter was added on the back focal plane of L2. The reconstructed image is taken by a professional camera at a distance of 576 mm from the L3, which can also be viewed directly by the human eye. The optical system is illustrated in Fig. 6.

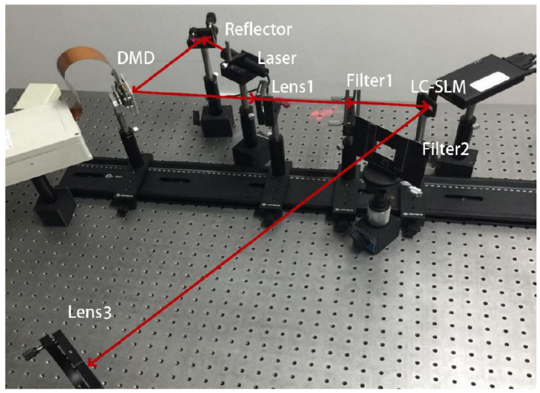

Fig. 6. Electronic holographic 3D display system.

The sub-holograms are sequentially loaded in the DMD, while the LC-SLM loads the corresponding phase diagram, projecting the sub-reconstructed images to different viewing zones. The experimental results are shown in Fig. 7. Figs.7(a)–(c) show the sub-holograms generated by

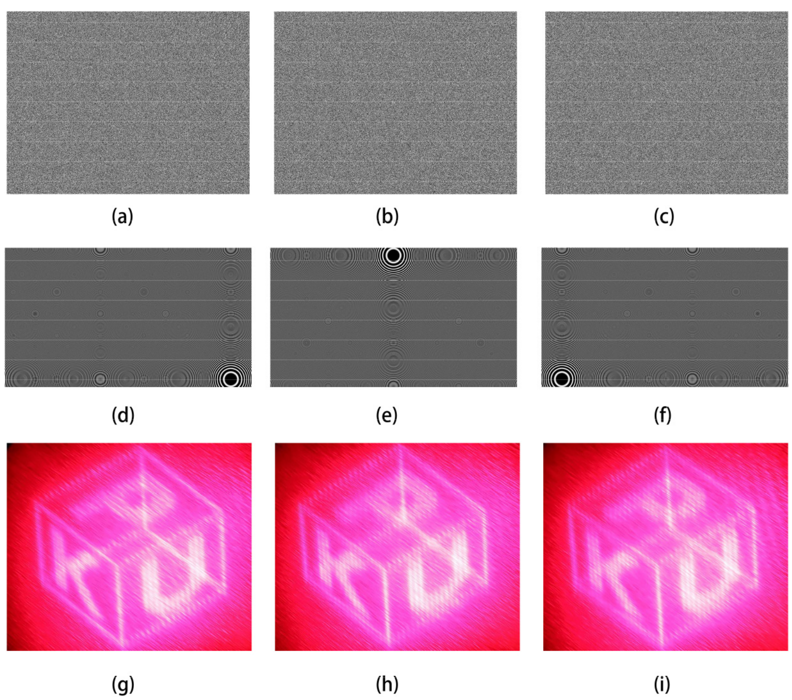

Fig. 7. Electronic holographic 3D display with three viewing zones of CGH7, CGH2, CGH9(Fig.3). (a)-(c) the generated sub-holograms, (d)-(f) phase diagrams of the off-axis Fresnel lenses loaded by the LC-SLM,(g)-(i) reconstructed images.

OSA CONTINUUM

the point-source-based method at the positions of CGH7, CGH2, CGH9 (Fig. 3) respectively. Figs. 7(d)–(f) show the corresponding phase diagrams of Fresnel lens with different positions of the lens axis(left, middle and right) loaded by the LC-SLM. When the refresh rate of the DMD is aligned with that of the LC-SLM, the reconstructed images at different viewing zones are shown in Figs. 7(g)–(i).

The display size of the cube is $50\text{mm} \times 50\text{mm} \times 50\,\text{mm}$. When imaging with a bare DMD, the actual measured viewing angle of a single hologram is 0.6°, taken by the professional camera at the position of the LC-SLM. The experiments showed that the viewing angle of a single hologram is 0.6°. For the letters "PKU", using the proposed method, the viewing angles along both horizontal and vertical directions were extended to 2.2°. Compared with the single hologram, the viewing zone is enlarged. Therefore, the experimental results showed that the non-mechanical scanning method using a phase-only LC-SLM can increase the viewing angle of the electronic holographic 3D display system.

5. Conclusion

A method to enlarge the viewing zones of the electronic holographic 3D display system was proposed. Real 3D objects could be recorded and reconstructed using the point-source-based method. In the experiments, a phase-only LC-SLM was used to simulate the off-axis Fresnel lenses in order to deflect the reconstructed light. The reconstructed images were projected to different positions to expand the viewing zones. The viewing angles along both horizontal and vertical directions were extended to 2.2°; therefore, the proposed method can be used to increase the viewing angle of the electronic holographic display system. Although the reconstructed images did not have a very high quality, we could display relatively large 3D images in electronic holography. In future studies, we aim to improve the quality of the reconstructed images.

Funding

National Natural Science Foundation of China (NSFC) (61271310).

References

1. B. Javidi, F. Okano, and J. Y. Son, *Three-dimensional Imaging, Visualization, and Display* (Springer, 2009).
2. G. Finke, T. Kozacki, and M. Kujawińska, "Wide-viewing-angle holographic display with a multi-spatial light modulator array," Proc. SPIE, **7723** 77230A (2010).
3. J. Hahn, H. Kim, Y. Lim, G. Park, and B. Lee, "Wide-viewing-angle dynamic holographic stereogram with a curved array of spatial light modulators," Opt. Express **16**(16), 12372 (2008).
4. H. Y. Chen and T. D. Wilkinson, "Field of view expansion for 3-D holographic display using a single spatial light modulator with scanning reconstruction light," in *3DTV Conference: The True Vision-Capture, Transmission, and Display of 3D Video* , (IEEE, 2009), pp. 1–4
5. Y. Z. Liu, X. N. Pang, S. Jiang, and J. W. Dong, "Viewing-angle enlargement in augmented holographic reality using time division and spatial tiling," Opt. Express **21**(10), 12068–12076 (2013).
6. D. Teng, L. Liu, Z. Wang, B. Sun, and B. Wang, "All-around holographic three-dimensional light field display," Opt. Commun. **285**(21-22), 4235–4240 (2012).
7. H. E. Kim, M. Park, K. Moon, and J. W. Kim, "Table-top three-dimensional holographic display using ellipsoid mirror," *Proc. 3DSA 2014 Korea* (3DSA, 2014), pp. 4–15
8. T. Inoue and Y. Takaki, "Table screen 360° holographic display using circular viewing-zone scanning," Opt. Express **23**(5), 6533 (2015).
9. J. P. Waters, "Holographic image synthesis utilizing theoretical methods," Appl. Phys. Lett. **9**(11), 405–407 (1966).
10. M. E. Lucente, "Interactive computation of holograms using a look-up table," J. Electron. Imaging **2**(1), 28–34 (1993).
11. S. C. Kim and E. S. Kim, "Effective generation of digital holograms of three-dimensional objects using a novel look-up table method," Appl. Opt. **47**(19), D55 (2008).
12. P. F. Mcmanamon, P. J. Bos, M. J. Escuti, and E. A. Watson, "A review of phased array steering for narrow-band electrooptical systems," Proc. IEEE **97**(6), 1078–1096 (2009).
13. Y. Hao, Y. Huang, Q. Wu, and W. Xiao, "The research of methods to improve the control bandwidth for liquid crystal beam steering system," Proc. SPIE **8906**, 89061T (2013).

OSA CONTINUUM

14. S. Serati and J. Harriman, "Spatial light modulator considerations for beam control in optical manipulation applications," Proc. SPIE **6326**, 63262W (2006).
15. P. Mcmanamon, "An overview of optical phased array technology and status," Proc. SPIE **5947**, 59470I (2005).
16. P. Q. Lin, C. F. Ying, Z. B. Xu, H. Pang, and F. Lou, "Implementation of the controllable zoom lens based on phase-only liquid crystal spatial light modulator," J. Appl. Optics **31**(3), 376–380 (2010).
17. J. Q. Qu, L. M. Zou, Y. J. Chen, and X. M. Ding, "Realization of non-mechanical lateral and axial confocal microscopic laser scanning with a phase-only liquid-crystal spatial light modulator," Key Eng. Mater. **613**, 167–172 (2014).
18. L. Shi, J. Shi, P. F. McManamon, and P. J. Bos, "Design considerations for high efficiency liquid crystal decentered microlens arrays for steering light," Appl. Opt. **49**(3), 409–421 (2010).
19. J. L. Gibson, B. D. Duncan, E. A. Watson, and J. S. Loomis, "Wide-angle decentered lens beam steering for infrared countermeasures applications," Opt. Eng. **43**(10), 2312–2321 (2004).
20. D. Engström, J. Bengtsson, E. Eriksson, and M. Goksör, "Improved beam steering accuracy of a single beam with a 1D phase-only spatial light modulator," Opt. Express **16**(22), 18275–18287 (2008).